Applied Thermal Engineering 243 (2024) 122652

Contents lists available at ScienceDirect

Applied Thermal Engineering

journal homepage: www.elsevier.com/locate/ate

Research Paper

Field study of a direct absorption solar collector with eco-friendly nanofluid

Pavel G. Struchalin [a,*], Yansong Zhao [b], Boris V. Balakin [a]

[a] Department of Mechanical and Marine Engineering, Western Norway University of Applied Sciences, Inndalsveien 28, Bergen, 5063, Norway
[b] Department of Safety, Chemistry and Biomedical Laboratory Sciences, Western Norway University of Applied Sciences, Inndalsveien 28, Bergen, 5063, Norway

ARTICLE INFO

Keywords:
Direct absorption solar collector
Nanofluid
Organic
Solar thermal
Field study

ABSTRACT

The concept of direct absorption solar collector (DASC) was introduced in the 1970s. Multiple laboratory studies proved that nanofluid-based DASCs presented a fruitful alternative to conventional solar collectors. However, due to environmental and cost limitations of nanofluids, there are few records of real-size DASCs operating in field conditions. Filling the gap, we report a 5-month seasonal field study for a full-scale DASC with an eco-friendly and low-cost nanofluid. Throughout the experiments, the DASC competed with a commercial flat-plate solar collector mounted in the exact location. The results showed that the commercial collector had an average daily efficiency of about 65.9%, while the direct absorption collector had a daily efficiency of 57.7% to 86.1%. The most important parameters influencing the efficiency of the DASC are the flow rate and the extinction coefficient of the nanofluid. They alter the efficiency by 9.2% and 6.2%. Finally, the article briefly notes the technical and economic features of the DASC operation.

1. Introduction

One of the critical problems of conventional solar thermal technology is the high superheating of the surface absorbing solar radiation and, as a result, high thermal leaks to the environment [1]. In recent decades, direct absorption of solar energy in the heat transfer fluid, bypassing the stage of receiver heating, has been actively studied [2]. Nanofluids are proposed for direct absorption systems as heat transfer fluids and absorbers of solar radiation [3]. Active research demonstrated that direct absorption solar collectors (DASC) outperform solar collectors of a standard design [4,5]. This has been confirmed both on a laboratory scale and a field scale.

Minardi and Chuang [6] carried out the pioneering prototype study of the DASC based on inks and aquadag-fluids with microscopic particles. The lab-scale solar collector (~0.6 m^2) was tested outdoors for five days. High values of thermal efficiency (57.3–79.6%) were obtained during the tests. However, spiral-tube flow channels were used to encapsulate the opaque fluid, which could have resulted in a high-pressure drop. Moreover, the utilized microscopic particles were not entirely stable in the collector and contaminated the internal surface of the transparent surfaces. Following the inception work on the direct absorption solar collector [6], nanofluids were pointed out as more stable optical absorbers for DASCs [7]. Dozens of lab-scale experiments with DASCs based on nanofluids are documented in the literature; detailed overviews of these works may be found in [8,9]. In these studies, the usage of aqueous nanofluids with nanoparticles of Au [10], CuO [11], multi-walled carbon nanotubes (MWCNTs) [12], and Fe_3O_4 [13] resulted in maximum thermal efficiencies in the interval 40%–95%. Detailed experimental and numerical studies of a tubular prototype DASC were presented by Struchalin et al. [8,14]. This work examined a tubular DASC of 0.49 m^2 using aqueous nanofluids with different concentrations of MWCNTs and nanoparticles of Fe_3O_4. Although the average thermal efficiency of the collector was in the interval 60%–80%, this collector was not tested in realistic climate conditions. None of the DASC experiments from the literature reported an industry-relevant prototype of about 2 m^2, and the design of the collectors was not optimized in terms of thermal performance and pumping costs.

On the way of commercialization of this technology, the problem of nanofluid toxicity arises. Elsaid et al. [15], summarizing different research results, discussed that many types of nanoparticles considered candidates for use in DASC had an adverse biological and environmental impact. For instance, this is related to metals, their oxides [16], and carbon-based nanoparticles [17]. The nanoparticles may stick to, disrupt the functioning, or damage the body cells, and produce harmful ions [18,19]. Maximum safe concentrations of these nanoparticles are deficient: the values are up to tens of micrograms per m^3 [15].

The further development of nanofluid technology requires creating an environmentally friendly and biodegradable alternative. At present, this stage of technology is only developing. To date, $Ti_3C_2T_x$ MXene/water [20], $CoFe_2O_4$/rGO/water [21], functionalized GNP/water [22], Ag/coconut oil [23] have been purposed for heat transfer applications; SiO_2, WO_3/Neem oil [24], silica oxide/corn oil [25] nanofluids

* Corresponding author.
E-mail address: pstr@hvl.no (P.G. Struchalin).

https://doi.org/10.1016/j.applthermaleng.2024.122652
Received 5 September 2023; Received in revised form 24 December 2023; Accepted 4 February 2024
Available online 6 February 2024

are considered as promising materials. Regarding the solar energy application, water dispersion of graphene nano pellets [26,27], MWCNTs [28], titanium and silica dioxide nanoparticles synthesized by using olive leaf extract and barley husk [29] have been studied. Direct absorption of solar energy for thermal application was considered in the work of Gupta et al. [30], who used the dispersion of gold nanoparticles in Azadirachta Indica leaf extract.

However, the safety of the nanofluids mentioned above is questionable because they still contain nanoparticles with low safe concentrations, albeit dispersed in a neutral medium. Furthermore, the biological tests of the listed nanofluids were not performed. The best way to produce an eco-friendly nanofluid is the simultaneous use of non-toxic particles and a dispersing medium. The number of studies regarding such kinds of nanofluids is noticeably low. We note a few works related to the direct absorption of solar energy.

A significant contribution was made by Alberghini et al. [31]. The authors prepared a colloid based on distilled water and microparticles of Arabica coffee, which were mixed with glycerol and copper sulfate. The resulting concentrate was diluted with water in different proportions. For testing the photothermal properties of the obtained fluid, a lab-scale solar collector was used, covered on the top with either a transparent wall (for colloid tests) or an opaque receiver (for a test with a standard water coolant). As a result, the best performance of the collector with the transparent receiver was achieved using a 50:50 mixture of colloid concentrate with water. In this case, the collector's performance was 3.0–5.9% higher than with the opaque receiver.

A similar coffee colloid was considered for solar desalination purposes. In the work of Essa et al. [32], micrometer-sized coffee particles were introduced into salty water distributed on a flat surface under a transparent cover. This case was compared with the standard conditions when salty water evaporated on a black-painted surface. The design of both solar stills was the same, and all internal surfaces were painted black. A 12-h outdoor test under natural sun irradiation showed that adding coffee particles to the salty water increased the solar still productivity by 35.14%. Kosinska et al. [33,34] also studied brewed coffee colloids for photo-thermal conversion applications. Three different liquids were heated by thermal radiation: distilled water, brewed coffee water colloid with no chemical additions, and carbon black/water nanofluid stabilized by sodium dodecyl sulfate (SDS). As a result, coffee colloid and carbon-based nanofluid showed better light absorbance than water, having the final temperature increase of 51.8 and 48.7 °C, correspondingly, after 5100 s of heating. However, it is seen that used coffee colloid had lower performance than nanofluid. In the following work [34], the outdoor experiments were carried out. Here, the natural sunlight heated static samples of the coffee colloid and the nanofluid in a dish solar concentrator. The result was similar to that of the previous study. The nanofluid sample absorbed solar light with higher efficiency. In these works [33,34], the sizes of coffee particles lie in the micrometer range, which can lead to a loss of colloid stability and deposition. Although not nanofluids, they were developed for the same purpose: directly converting solar radiation energy into heat in a coolant.

Further development of the coffee-containing fluids was demonstrated in the work of Balakin et al. [35]. Instead of brewed coffee, this study proposed using instant coffee granules, additionally sonicated and stabilized with 0.1% wt. of SDS. Granulometric analysis showed that various commercial brands of instant coffee could be used for the production of nanofluids with an average particle size of about 100 nm. Balakin and Struchalin [35] conducted toxicity tests (Daphnia Magna) for the developed nanofluid. The test showed toxicity at standard heat transfer fluids' level.

Gupta et al. [36] proposed an alternative biodegradable nanofluid based on *Azadirachta Indica* extract. In this work, fresh leaves were boiled in ethanol. The resulting extract was mixed with water in various proportions and subjected to the standard photothermal test of heating static fluid samples with light. Distilled water was used as a reference liquid. As expected, the colored fluid absorbed light more intensively.

Fig. 1. Flat-plate (left) and DASC (right) mounted on site.

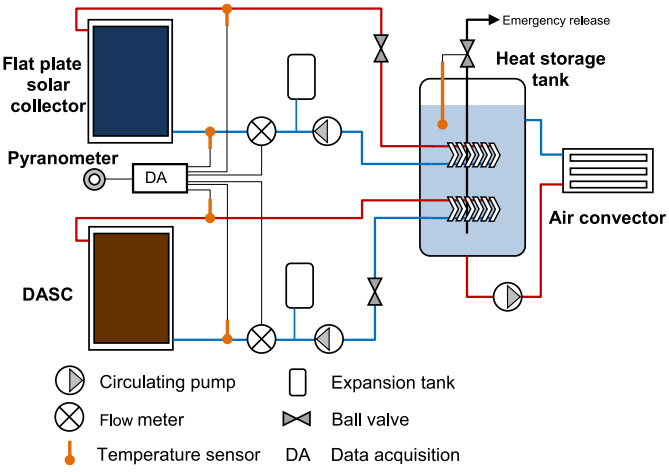

Fig. 2. Flowchart of the experimental system.

A short series of tests led to more significant heating of the colored fluid than transparent water. However, the lifecycle of the purposed fluid was short due to the rapid degradation of chlorophyll. The colored fluid became noticeably blanched after 6 h of exposure to sunlight. When the samples were heated for 2 h, the fluid was 13% more efficient than water (55% vs. 42%). However, during a 6-h test, this difference decreased down to 2% (40% vs. 38%). This colored fluid would not be able to outperform standard solar collector technology.

As can be seen, investigations of fully biodegradable nanofluids for photo-thermal applications are premature. Despite the apparent safety of the proposed environmentally friendly nanofluids, the results of toxicological tests are given in a few works [35]. In addition, at the moment, the literature lacks data on long-term performance tests in realistic conditions of the collectors with such nanofluids.

This work aims to perform a seasonal performance test of an industry-relevant prototype of a direct absorption solar collector using an instant coffee-based nanofluid reported in [35]. We present the design of the prototype and describe its performance. The article demonstrates how the thermal performance of the DASC can be changed using hydraulic regulation, altering thermal insulation, and the opacity of the nanofluids. In addition, we compare the performances of the direct absorption collector and a commercial model of the most available type of solar collector (flat-plate solar collector) in the same conditions. The experiments were conducted under Northern climate conditions.

Table 1
Experimental equipment.

Components	Type, producer	Specifications
DASC	Odda Plast AS (Norway)	Max. fluid temp.: 80 °C Max. fluid pressure: 0.2 bar Absorber area: 1.51 m^2 H × W × T: 2151 × 1170 × 84 mm Weight (dry/wet): 80.0/95.7 kg
Flat-plate solar collector	KPG1-ALC, Regulus (Czech Republic)	Max. fluid temp.: 120 °C Max. fluid pressure: 10 bar Absorber area: 2.31/1.77 m^2 (Std/Test) H × W × T: 2151 × 1170 × 84 mm Weight (dry/wet): 47.0/48.7 kg
Temp. sensor	FKP5.5 Pt1000, Resol (Germany)	Meas. interval: −50–180 °C Err.: ±0.3–0.8 °C (0–100 °C) Resolution: 0.1 °C
Flow meter	V40-15, Resol	Meas. interval: 1–50 l/min Resolution: 0.1 l/min
Pyranometer	SP Lite 2 Kipp & Zonen (Netherlands)	Spectral range: 400–1100 nm Sensitivity: 75.4 μV/(W/m^2) Maximum solar irradiance: 2000 W/m^2
Pressure gauge	Analog	Max. pressure: 2 bar Resolution: 0.05 bar
Data acquisition	DL3, Resol (Germany) CR310, Campbell Scientific (USA)	Temperature, flow rate solar irradiation
Collector's pump	Star-RS 15/6, Wilo (Germany)	Max. flow rate: 4.6 m^3/h Max. head: 5.5 m
Heat storage tank	Fish 300 S2, Sunex (Poland)	Capacity: 300 l
Secondary pump (greenhouse)	Yonos PICO 25/1-4, Wilo (Germany)	Max. flow rate: 2.7 m^3/h Max. head: 4 m
Pipes		∅22 × 1 mm, Copper

2. Experiments

Experimental facility

The efficiency study of a direct absorption solar collector with a biodegradable nanofluid was conducted in Bergen, Norway, from May to September 2022. Our test facility comprises two solar collectors and a technical house with flow equipment. The facility, shown in Fig. 1, is outdoors at Western Norway University of Applied Sciences (60° 22004.200 N 5° 21003.300 E). Popsueva et al. [37] present more details about the facility. The set-up diagram is presented in Fig. 2. The collectors are connected to an individual hydraulic loop. According to the manual for the commercial solar collector [38], both collectors are placed on a metal frame at the angle of 45° to the horizon. All the heat absorbed by DASC is transferred to a heat storage, a domestic hot water tank, through a coil heat exchanger immersed in the tank. The tank is a 300-L cylindrical volume, having an additional circulation loop transferring heat to convectors heating a greenhouse. For a referent comparison of DASC performance, a commercial flat-plate solar collector (FPC) is used on-site. It is mounted next to the DASC and connected to another individual circulation loop closed on the second heat exchanger of the storage tank. During the experiments, both collectors operated under equivalent climate conditions. Although the area of the DASC and the FPC differ by 0.26 m^2, the referent collector is the closest available analog. The equipment used in the flow loops is the standard for solar facilities and the same for both collectors. Table 1 presents detailed information on the installed equipment.

The experimental procedure was as follows. Before the start of the experiment, the desired pumping power was set equal for both collectors. The experiment started in the morning when the rising sun began to create a light flux sufficient for the appearance of detectable liquid heating in the collectors. This moment of time was the same for both collectors. During the day, the temperatures of the liquid at the inlet, t_{in}, and outlet, t_{out}, of the collectors, the volumetric flow rate of the liquid, f_v, and the solar radiation normal to the collectors' surface, I, were recorded. An example of the experimental logs for both the collectors is shown in Fig. 3.

Based on the measured data, the total daily absorbed thermal energy, Q_t, by the collectors was determined by Eq. (1), and the total amount of incoming light energy, Q_i, was determined by Eq. (2):

$$Q_t = \sum_i \rho_i f_{v,i} c_{p,i} (t_{out,i} - t_{in,i}) \tau_i, \tag{1}$$

$$Q_i = \sum_j A I_j \tau_j, \tag{2}$$

where ρ, c_p are the density and heat capacity of the heat transfer fluid, A is a collector's absorber area, I is the light energy flux on the absorber plane, τ is the data acquisition time step $\tau_i = 10$ s for the temperature and flow rate data, and $\tau_j = 120$ s for the solar radiation. Then, the average daily efficiency of the collector, η, is determined as the ratio of Eqs. (1)–(2):

$$\eta = \frac{Q_t}{Q_i} \tag{3}$$

The time to complete the thermal energy collection for the collectors varied due to the significant difference in the heat capacity of materials used in the collectors. The temperature gradient in the FPC became negative several minutes after the solar radiation stopped. In contrast, due to the accumulated heat, the direct absorption solar collector continued to heat the coolant for another 5-8 h after sunset.

Nanofluid

The direct absorption solar collector utilized a coffee-based nanofluid described in Balakin and Struchalin [35]. The nanofluid is inexpensive and has low toxicity values in *Daphnia magna* test. We used a commercial instant coffee distributed in Norway to produce the nanofluid. The required mass of coffee was first dissolved in hot water at 95 °C, then cooled to room temperature and treated by ultrasound for

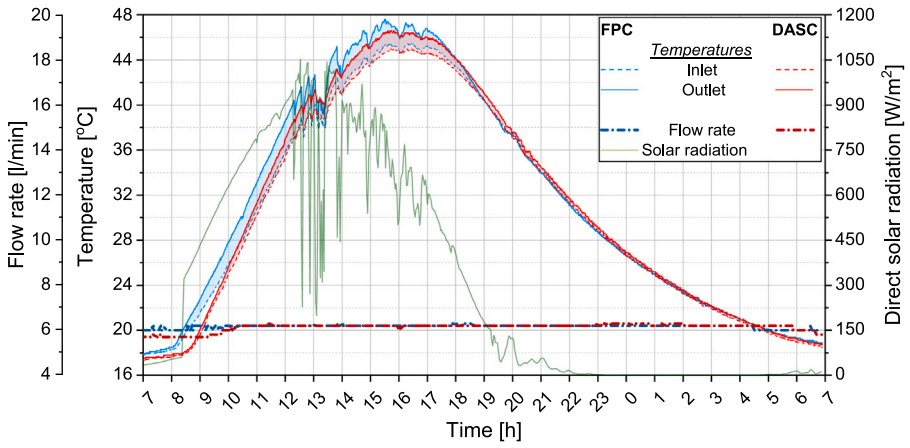

Fig. 3. Example of the experimental logs (20.06).

20 min using an immersion disperser (MEF93.T from MELFIZ, 600 W, 22 ± 1.65 kHz). The agglomeration of nanoparticles was prevented by the addition of 0.1% wt. of sodium dodecyl sulfate (99%, Sigma Aldrich). To verify the stability of the nanofluid, a dilute droplet with 0.2% of particles was dried and studied microscopically using Zeiss Gemini 450 scanning electron microscope. Twelve hours after the production, the resulting nanofluid's optical property (extinction coefficient) was determined, and then, the nanofluid was charged into the DASC. The nanofluid was mixed with the base fluid or a more concentrated nanofluid to tune up the extinction coefficient in the DASC.

The nanofluid's extinction coefficient κ was determined by light transmission measurements performed by a spectrophotometer UV-5100B (Metash) in the wavelength range of 370–900 nm. The extinction coefficient of the fluid and the light transmittance T depend on the wavelength λ. For engineering applications, this requires the introduction of an average extinction coefficient κ_{av}:

$$\kappa_{av} = \frac{1}{\lambda_{max} - \lambda_{min}} \cdot \int_{\lambda_{min}}^{\lambda_{max}} \kappa(\lambda)\, d\lambda, \tag{4}$$

where λ_{min} and λ_{max} are the minimum and maximum wavelength of light irradiating a liquid sample in a spectrophotometer, correspondingly.

However, when an optical system is exposed to natural sunlight with an uneven spectrum, the average extinction obtained by Eq. (4) may not reflect its absorption ability. Therefore, we define an additional effective extinction coefficient κ_{eff} considering natural solar spectrum [39]:

$$\kappa_{eff} = -\frac{1}{l} \cdot ln\left(\frac{\int_{\lambda_{min}}^{\lambda_{max}} I(\lambda)\, d\lambda}{\int_{\lambda_{min}}^{\lambda_{max}} I_0(\lambda)\, d\lambda} \right), \tag{5}$$

where $I_0(\lambda)$ and $I(\lambda)$ are the powers of the incident and transmitted through liquid sunlight (W/(m^2 nm)), correspondingly, l is the thickness of fluid sample during its measurement with a spectrophotometer. We calculated transmitted radiation using the instantaneous values of κ and then numerically solved terms in Eq. (5).

Data on the nanofluid's viscosity were required to calculate the pumping losses. The viscosity of the nanofluid was measured using a standard Couette viscometer NDJ-8S (rotor № 0, ±0.1 mPa s) in the temperature range of 25–80 °C. Thermal stabilization was performed using a custom water bath with temperature stability within ±2 °C. Temperature control was carried out using a K-type thermocouple connected to the RS-PRO datalogger.

2.1. DASC design

The design of the DASC is similar to that of a standard flat-plate solar collector. The flat-plate collector has a series of parallel copper pipes through which the coolant flows. A "blackened" thin metal sheet is welded to these pipes, thus transferring absorbed heat. From the back and sides, the channels are surrounded by thermal insulation and collector housing. From the front side, the absorber and pipes are covered with glass. More details on the design of standard FPCs are available in Duffie and Beckman [40].

The design of DASC (Fig. 4) differs in that the channels are combined with the absorber. In the internal volume of the DASC, three flat and wide parallel channels are formed where the nanofluid flows. The channels are formed by two 1-cm baffles. The width of the gaps is 28 cm. The baffles form 2-cm openings towards the top and bottom walls of the casing to enable the horizontal circulation of the nanofluid. The front wall of the channels is transparent. The casing of the DASC is 3 cm thick, it is made of high-density polyethylene (PE300). The transparent wall is made of a 1 cm thick polycarbonate sheet. The polycarbonate wall is sealed against the casing using elastomer. The polycarbonate is mounted and pressed by M8 × 60 hex bolts. The collector is inserted in a thermal insulation case (extruded polystyrene foam), having thermal resistance equivalent to that of the FPC's thermal insulation (~0.75 m^2 K/W). From the front side, the DASC is covered with a second transparent polycarbonate sheet, which forms a thermally insulating air gap of 1 cm thick between the transparent surfaces. Both transparent surfaces are designed to be removable. The collector and the heat-insulating casing were installed in the grooves of the plastic base plate used to fix the collector on a metal frame. The connection ports of the DASC are 3/4″. The resulting absorbing area of the channels is 1.51 m^2, and the dry mass of the collector is 80 kg. The fluid volume in the DASC was 15.7 l, nine times higher than the volume of fluid used in the FPC.

Experimental uncertainties

Experimental uncertainties of the thermal efficiency were calculated through the standard technique for combined uncertainties (6):

$$\Delta\eta = \sqrt{\left(\frac{\partial\eta}{\partial Q_t}\right)^2 \cdot \Delta Q_t^2 + \left(\frac{\partial\eta}{\partial Q_i}\right)^2 \cdot \Delta Q_i^2} = \sqrt{\left(\frac{1}{Q_i}\right)^2 \cdot \Delta Q_t^2 + \left(\frac{Q_t}{Q_i^2}\right)^2 \cdot \Delta Q_i^2}, \tag{6}$$

where ΔQ_t and ΔQ_i are uncertainties of collected thermal and total incident light energy:

$$\Delta Q_t = \sum_i \Delta Q_{t,i}, \tag{7}$$

$$\Delta Q_i = \sum_j \Delta Q_{i,j}, \tag{8}$$

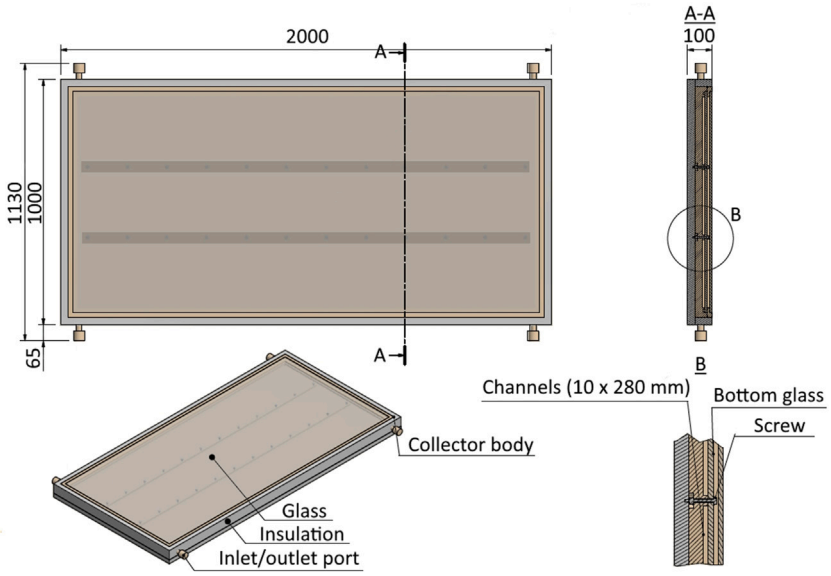

Fig. 4. Direct absorption solar collector.

where the instantaneous values of uncertainties are taken at different ith (thermal) and jth (incident) data acquisition time steps. These uncertainties are calculated as:

$$\Delta Q_{t,i} = \sqrt{\left(\frac{\partial Q_{t,i}}{\partial f_{v,i}}\right)^2 \cdot \Delta f_{v,i}^2 + \left(\frac{\partial Q_{t,i}}{\partial t_{r,i}}\right)^2 \cdot \Delta t_{r,i}^2}, \quad (9)$$

$$\Delta Q_{i,j} = \frac{\partial Q_{i,j}}{\partial I_j} \cdot \Delta I_j, \quad (10)$$

where $t_{r,i} = t_{out,i} - t_{in,i}$, $\Delta f_{v,i}$ and $\Delta t_{r,i}$ are taken equal to the resolution of the data acquisition by the datalogger DL3, and ΔI_j is the instrumental error of the pyranometer, equal to 5% of the measured value [41]. Uncertainties of thermal properties, time acquisition, and absorber areas were not considered as they were negligibly low.

3. Results and discussion

Nanofluid

This follows from the prior SLS study of the nanofluid [35] that the number-average particle size is 90 nm in liquid. In Fig. 5, we present the results of scanning electron microscopy conducted for a dried nanofluid sample. The figure shows that the particle sizes are about twice as low as the hydrodynamic sizes obtained from the SLS. We also note that the process of drying the sample could contribute to the thermal fragmentation of the particles.

The analysis of the results should be carried out by referring to the relevant properties of the nanofluid. In similar works devoted to studying DASCs (e.g.[7,8]), the collectors' performance is correlated with the particle concentration in the nanofluid used in the test. In this work, we proposed an alternative method relating the performance of the DASC with the extinction of the nanofluid. This approach is more pragmatic from the operation viewpoint because it describes the optical properties of the system directly. In Table 2, we demonstrate how the extinction in our nanofluid is related to the concentration of particles.

As seen from Table 2, the extinction coefficient corrected for the solar spectrum is, on average, 39% lower than the wavelength-average extinction coefficient as the maximum absorption is shifted from the maximum of the solar spectrum. Measurements of the light transmission of the used polycarbonate showed a uniform and slight attenuation of the light power in the wavelength range of 370–900 nm. This made it possible to consider that the natural solar spectrum is not significantly deformed when passing through polycarbonate. An example of the light transmission spectrum of polycarbonate, as well as newly-produced nanofluid samples, is shown in Fig. 6. We did 48-h stability tests of these nanofluids. The resulting reduction of the effective extinction was lower than 3% during the tests. In further analysis of the results, we will use the effective extinction coefficient, which considers the shape of the solar spectrum.

Table 2
Averaged (κ_{av}) and solar-spectrum-corrected (κ_{eff}) extinction coefficient of newly-produced nanofluids.

x_{in} [% wt.]	0.1	0.2	0.5	1.0	2.0
κ_{av} [1/m]	45	86	181	276	397
κ_{eff} [1/m]	30	52	98	159	270

Fig. 6 also shows that the absorption spectrum of the nanofluid is non-uniform, increasing with a shift to the violet and ultraviolet regions of the spectrum. On the contrary, the uniform absorption spectrum, closest to which graphite nanofluids have, can be considered more optimal. We do, however, note that the maximum price for the production of our nanofluid is under 53 NOK, which is at least 485 times lower than the commercial nanofluids described in Chavez Panduro et al. [42] and of the same price order as many of conventional heat transfer fluids and an in-house carbon-based nanofluid developed by Struchalin et al. [8]. More details on nanofluid production costs are presented in supplementary materials.

DASC performance

The results of the DASC performance experiments are summarized in Fig. 7. It presents the average daily efficiency of the flat-plate and direct absorption solar collector on different days of the test season. The average daily coolant flow rate accompanies these data, the amount of collected heat energy, and the nanofluid extinction coefficient. We note that at the initial stage, the extinction of the nanofluid was measured 12 h before the start of the experiment. However, the fresh nanofluid darkens in contact with copper elements of the loop, increasing the effective extinction by 96.8%. Therefore, starting from August 28, the extinction of the nanofluid was controlled and altered based on samples taken from the set-up after the nanofluid reacted with copper. The extinction coefficients shown in Fig. 7 before this date are estimated by twice increasing values for freshly produced nanofluids.

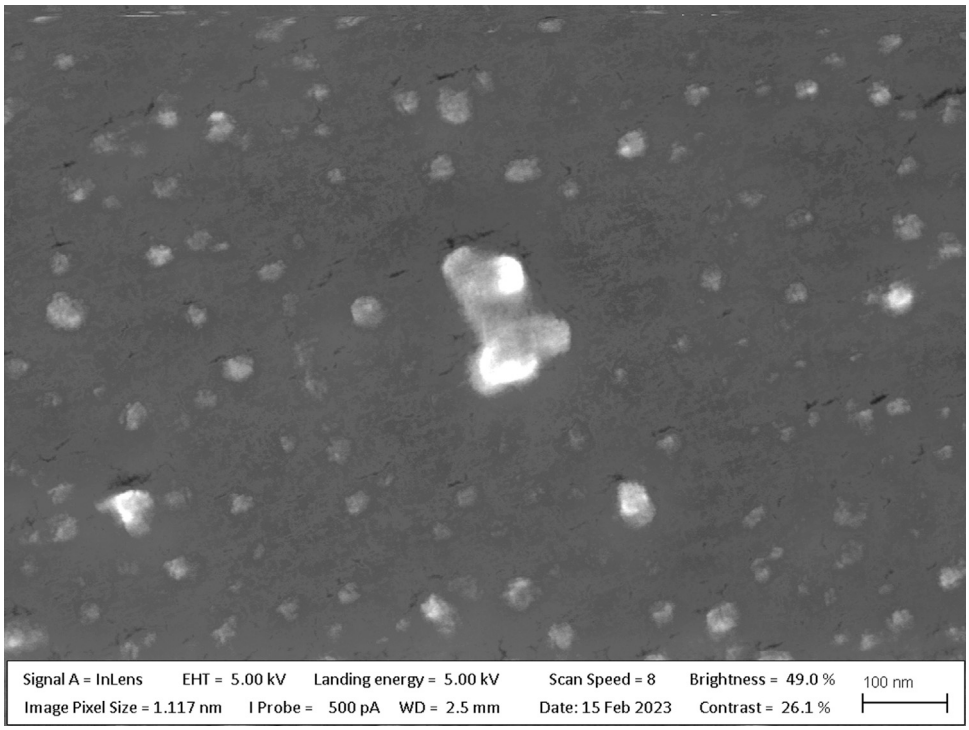

Fig. 5. Microscopy of the dry nanofluid sample.

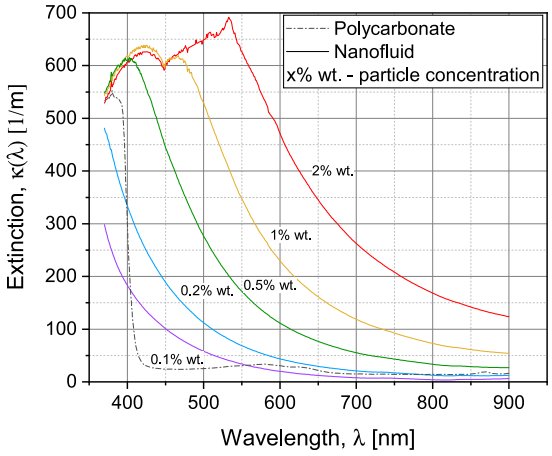

Fig. 6. Extinction coefficient of nanofluid and polycarbonate.

A typical domestic dwelling consumes about 100 MJ of heat [37]. This corresponds to the production of at least four commercial FPCs. According to the manual, the operation point of such a system includes an average flow rate of 8 l/min [38]. In this study, we altered the flow rate around the set point to examine the sensitivity of the collectors to the flow rate. We also note that the flow rates differ slightly between the DASC and FPC. This is explained by different flow resistances in the hydraulic circuits of the collectors, which is due to space limitations.

Fig. 7 shows that from May 16th to September 10th, the average efficiency of the flat-plate solar collector was 65.9% (min. 59.4%, max. 84.5%). The maximum efficiency corresponds to the weather conditions that limit thermal loss from the collector yet deliver a significant amount of radiant heat. The variation of the coolant flow rate within 5.8–8.3 l/min slightly increased the flat-plate collector's efficiency. For example, when the flow rate had been changed from 5.8 to 8.3 l/min, it boosted the collector efficiency by 2.7%. The average temperature difference between the FPC and the ambient did not change significantly. The variation interval was from 13.1 to 25.2 °C, and these temperatures did not influence the collector's efficiency much. Throughout the test season, the flat-plate collector demonstrated stable efficiency that was in good agreement with the technical data provided by the manufacturer [38]. The daily amount of thermal energy collected by the flat-plate solar collector varied from 17.9 to 30.4 MJ, with 25 MJ produced on average.

The efficiency of the DASC demonstrated a different sensitivity to process and climate conditions. During the experiments, its efficiency varied between 57.7% and 86.1%. The harvested thermal energy by the DASC was 15.6–30.7 MJ, with 23 MJ on average. The flow rate of the nanofluid, varying in the range of 6.1–8.7 l/min, had a noticeable effect on the DASC's efficiency. This influence is depicted in Fig. 8, where we present the difference between the efficiencies of the DASC and the FPC for a fixed flow rate. In this figure, we present the difference in *percentage points* [43], i.e. using the *arithmetic* difference between the two efficiencies in percents. To simplify the further comparison between efficiencies, in the text below, % will refer to *percentage points*.

The comparison is made for the days when the solar irradiation and the temperature difference between the collector and the ambient were comparable for both collectors. However, the nanofluid flow rate in the DASC varied. As follows from the figure, at the flow rate of 6.1–6.2 l/min, DASC outperforms a flat-plate collector only by 1.3% on average. However, the DASC outperformed the FPC by 8.8% when the flow rate increased to 7.5–7.7 l/min and by 10.5% when the flow rate was 8.2–8.7 l/min. The higher efficiency of the DASC at a higher flow rate is due to the better mixing of nanoparticles in the DASC. This leads to the migration of frontal heated layers of liquid to the flow core, resulting in lower heat leaks. In addition, the high flow rate reduces the exposure time for the nanoparticles. This, again, leads to a lower average temperature and limits the thermal loss to the environment. At low extinction coefficients, an increase in the flow rate enhanced heat transfer with the bottom of the channels partially heated by the transmitted light. Similar results were obtained in the previous study for a lab-scale tubular direct absorption solar collector with a carbon-based nanofluid [8].

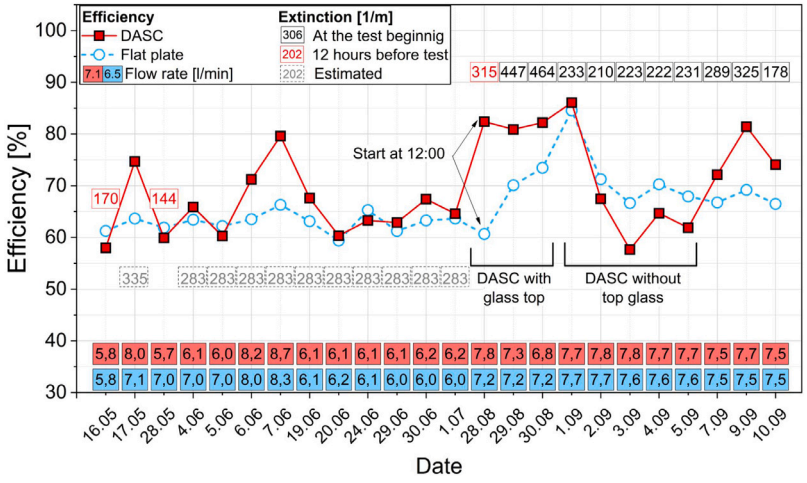

Fig. 7. DASC efficiency during the experimental season.

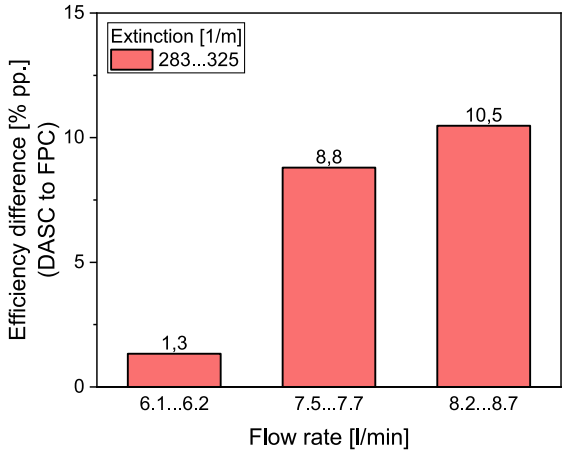

Fig. 8. Difference between the efficiencies of the DASC and the FPC for different flow rates. Data points taken on: 04/06, 05/06, 06/06, 07/06, 19/06, 20/06, 24/06, 29/06, 30/06, 01/07, 07/09.

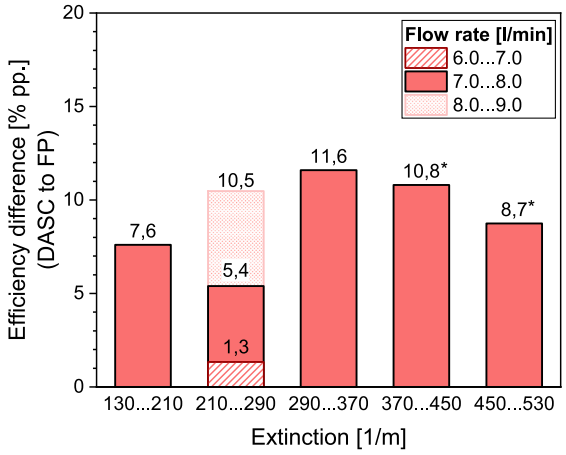

Fig. 9. Difference between the efficiencies of the DASC and the FPC for different extinction coefficients. Data points taken on: 17/05, 04/06, 05/06, 06/06, 07/06, 19/06, 20/06, 24/06, 29/06, 30/06, 01/07, 28/08, 29/08, 30/08, 07/09, 09/09, 10/09.

Another critical parameter that significantly affects the efficiency of the DASC is the extinction of the nanofluid. Previously, an optimal concentration of nanoparticles was detected and, therefore, an optimal value for the nanofluid extinction coefficient, providing the best efficiency of the DASC [8]. Low values of nanofluid's extinction lead to incomplete absorption of the incoming light energy, while high extinction leads to overheating of the nanofluid front layer, increasing heat losses. A similar result was obtained in the current study. Fig. 9 compares the efficiency of the flat-plate collector and the DASC with the nanofluid of different extinction. The nanofluid flow rate was comparable to those of the FPC, and its variation from day to day was insignificant (±0.2 l/min from the average value).

From Fig. 9, we read that the efficiency of the DASC is higher than that of a flat-plate collector by 1.3–11.6% in the entire range of nanofluid extinction considered (130–530 1/m). Moreover, the highest difference was achieved at 290–370 1/m extinction. The results for the extinction of 210–290 1/m demonstrate the flow rate's strong effect on DASC efficiency. At a flow rate of 6.0–7.0 l/min, DASC is 1.3% better than the FPC. However, when the flow rate was increased to 8.0–9.0 l/min, the DASC was 10.5% more efficient than the FPC. It should be noted that the DASC efficiency at the extinction of 210–290 1/m and flow rates 7.0–8.0 is lower (5.4%) than expected from the general data trend. This observation can be explained by the fact that a lower extinction leads to higher heating of the channel's back wall due to better light penetration through the nanofluid layer. From 5 to 14% of light energy can be absorbed in the backside of the duct. This partially changes the energy absorption mechanism in fluid from volumetric to surface type and potentially establishes a secondary convective flow intensifying mixing in the transversal cross-section. This effect possibly reduces when the extinction coefficient exceeds 210 1/m, and the DASC enters the volumetric absorption regime. We also note that the efficiency difference for the extinction ranges of 370–450 and 450–530 marked by "*" is taken from the tests with another type of transparent surface, tempered glass instead of polycarbonate, due to the lack of data. Despite that, we assume that the difference in efficiency would be lower if the polycarbonate surface was used in the experiments at the given extinction coefficient.

The design of the optical system is crucial for a direct absorption solar collector. In this regard, we additionally considered the effect of the top cover's material (glass/PC/none) on the DASC efficiency. In the primary case, DASC had two polycarbonate glasses. The inner glass is the channel wall in contact with the nanofluid, while the outer glass creates a thermally insulating air gap between the glasses. A standard solution for commercial collectors is tempered glass. In some cases, this glass can be supplied with an anti-reflective coating. In several tests, we modified DASC by replacing the outer polycarbonate glass with the standard tempered glass taken from another flat-plate collector.

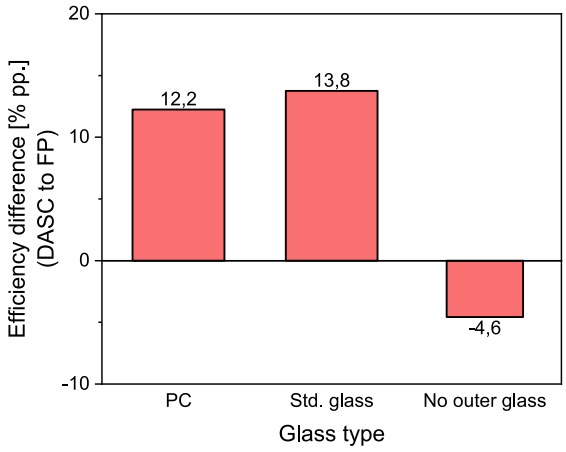

Fig. 10. Difference between the efficiencies of the DASC and the FPC for different top covers of the DASC. Data points taken on: 28/08, 29/08, 30/08, 01/09, 02/09, 03/09, 04/09, 05/09, 09/09.

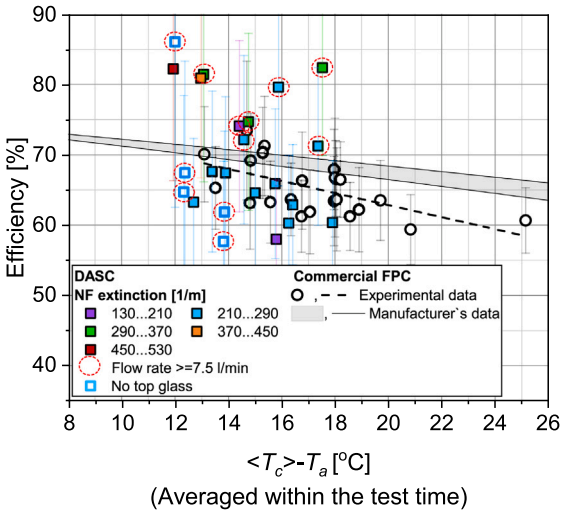

Fig. 11. Thermal efficiency of solar collectors as a function of the temperature difference between the collector and the environment.

It is matte and embossed, which can increase the back reflection of the irradiance reflected by the absorber before. The result of the modification is shown in Fig. 10.

It is seen that the modification of the transparent surface slightly increases the efficiency of the DASC. At the comparable level of the flow rates (7.3–7.7 l/min), the glass-covered DASC outperforms FPC by 13.8% while PC-covered DASC by 12.2% over the FPC. Despite this result, we assume that using both types of the DASC top makes it possible to obtain similar efficiency of the DASC if other conditions are regulated accordingly. We also tested whether an alternative optical system design for low-temperature collectors would be possible with no insulating air gap and removed the top glass accordingly. A lower light attenuation could compensate for the increased heat loss. However, the DASC has an efficiency 4.6% lower on average than the FPC when the top layer is absent.

Grade efficiency

Fig. 11 shows the grade efficiency plot for the flat-plate and the direct absorption solar collectors. Here, we present average data for cases with equivalent temperature differences between the collector and the environment. It is important to note that the previously presented Figs. 8–10 of the influence of flow rate, extinction, and glass material on the DASC-to-FPC efficiency analyzed the data obtained in the most similar conditions for both collectors (on the same day).

The experimental efficiency of the flat-plate collector was close to its technical data at irradiation in the 800–1000 W/m^2 [38], being lower by only 3.3%. This deviation can be explained by the fact that 24.4% of the absorber area was covered with an opaque screen for the experiments. At the same time, the overall collector's dimensions remained unchanged. Combining these two factors increased the ratio of heat loss to absorbed light energy, thus reducing the total efficiency of the collector.

As noted previously, the efficiency of the DASC is highly dependent on nanofluid extinction and flow rate. Fig. 11 shows that if extinction is in the range of 210–290 1/m, DASC is equivalent to the flat-plate collector in terms of efficiency. Only in case the coolant flow rate was set higher than 7.5 l/min, DASC outperformed FPC up to 13.2%. A noticeable increase in the DASC efficiency was observed when nanofluid extinction was over 290 1/m. In that case, DASC had an efficiency up to 17.4% higher than FPC.

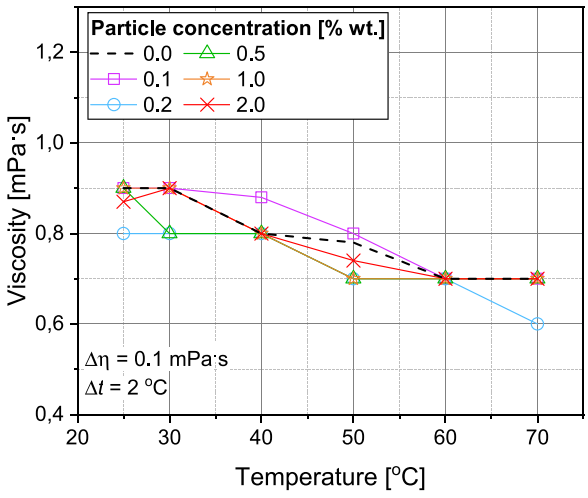

Fig. 12. Nanofluid viscosity.

Pumping costs

Analysis of the pumping cost in a collector system requires data on the density and viscosity of the coolant. We have measured the dynamic viscosity of the developed coffee nanofluid at various temperatures and concentrations. The results are shown in Fig. 12, where it follows that the viscosity of the base fluid (water and SDS) is similar to the viscosity of water; the viscosity reduces with temperature. The addition of particles and the following increase in their concentration increase the viscosity by a maximum of 7% relative to the base. The viscosity of the nanofluid is equivalent to the viscosity of water.

Due to the specifics of the plumbing network of the test facility, there was no technical opportunity to locate a differential manometer between the ports of the DASC. Therefore, this parameter was determined numerically using a CFD model of the collector. The model is described in more detail in the supplementary materials. The results of the simulation are presented in Table 3. This table also lists the water pressure drop in the flat-plate collector [38].

Table 3 shows that the direct absorption solar collector requires a similar pumping power to that of the flat-plate collector. For both collectors, the pumping costs are below 5 W, which is lower than the total pumping cost for the hydraulic loop [37].

Table 3
Collector pressure drop.

Flow rate [l/min]	4	6	8	10
ΔP_{FPC} [Pa]	193	337	519	731
ΔP_{DASC} [Pa]	138	304	542	832

4. Conclusions

A seasonal field performance study of the full-scale direct absorption solar collector with the eco-friendly nanofluid was conducted in the Northern climate conditions. It has been established that with the best combination of operating parameters, namely, the extinction coefficient and the nanofluid flow rate, the average daily efficiency of the DASC can be up to 17.4% higher compared to the commercial flat-plate solar collector with the surface heat absorption. The highest efficiency of DASC was achieved at nanofluid flow rates over 7.5 l/min and extinction in the range of 290–370 1/m. During the period of experiments, the efficiency of DASC varied between 57.7–86.1%. At the same time, if the nanofluid parameters were not optimal, the efficiency of the DASC was comparable to that of the flat-plate collector. The collector and the nanofluid demonstrated stable operation during the entire experimental period.

Despite the positive result, the studied solar collector and nanofluid possess the potential for further improvement. The developed design of the direct absorption solar collector is rather complex, considering the need to seal the entire perimeter of the transparent top surface. The nanofluids reacted with copper, increasing its extinction, though in a controlled fashion.

CRediT authorship contribution statement

Pavel G. Struchalin: Conceptualization, Data curation, Investigation, Methodology, Validation, Writing – original draft, Writing – review & editing. **Yansong Zhao:** Data curation, Methodology, Writing – original draft. **Boris V. Balakin:** Conceptualization, Investigation, Methodology, Supervision, Writing – original draft.

Declaration of competing interest

The authors declare the following financial interests/personal relationships which may be considered as potential competing interests: Boris V. Balakin reports financial support was provided by Research Council of Norway. Boris V. Balakin and Pavel G. Struchalin have patent #Nanofluid for use in solar collectors. UK Patent Application no. GB 2208368.7 pending to Vestlandets Innovasjonsselskap AS.

Data availability

Data will be made available on request.

Acknowledgments

This study was supported by the Research Council of Norway.

Appendix A. Supplementary data

Supplementary material related to this article can be found online at https://doi.org/10.1016/j.applthermaleng.2024.122652.

References

[1] S. Faisal Ahmed, M. Khalid, M. Vaka, R. Walvekar, A. Numan, A. Khaliq Rasheed, N. Mujawar Mubarak, Recent progress in solar water heaters and solar collectors: A comprehensive review, Therm. Sci. Eng. Prog. 25 (2021) 100981, http://dx.doi.org/10.1016/j.tsep.2021.100981.

[2] M. Sainz-Mañas, F. Bataille, C. Caliot, A. Vossier, G. Flamant, Direct absorption nanofluid-based solar collectors for low and medium temperatures. a review, Energy 260 (2022) 124916, http://dx.doi.org/10.1016/j.energy.2022.124916.

[3] K. Farhana, K. Kadirgama, M. Rahman, D. Ramasamy, M. Noor, G. Najafi, M. Samykano, A. Mahamude, Improvement in the performance of solar collectors with nanofluids – a state-of-the-art review, Nano-Struct. Nano-Objects 18 (2019) 100276, http://dx.doi.org/10.1016/j.nanoso.2019.100276.

[4] M. Hussain, S. Khawar Hussain Shah, U. Sajjad, N. Abbas, A. Ali, Recent progress in solar water heaters and solar collectors: A comprehensive review, Energies 15 (2022) 7101, http://dx.doi.org/10.3390/en15197101.

[5] A.K. Hamzat, M.I. Omisanya, A.Z. Sahin, O.R. Oyetunji, N.A. Olaitan, Application of nanofluid in solar energy harvesting devices: A comprehensive review, Energy Convers. Manage. 226 (2022) 115790, http://dx.doi.org/10.1016/j.enconman.2022.115790.

[6] J.E. Minardi, H.N. Chuang, Performance of a black liquid flat-plate solar collector, Sol. Energy 17 (3) (1975) 179–183.

[7] T.P. Otanicar, P.E. Phelan, R.S. Prasher, G. Rosengarten, R.A. Taylor, Nanofluid-based direct absorption solar collector, J. Renew. Sustain. Energy 2 (3) (2010).

[8] P. Struchalin, V. Yunin, K. Kutsenko, O. Nikolaev, A. Vologzhannikova, M. Shevelyova, O. Gorbacheva, B. Balakin, Performance of a tubular direct absorption solar collector with a carbon-based nanofluid, Int. J. Heat Mass Transfer 179 (2023) 121717, http://dx.doi.org/10.1016/j.ijheatmasstransfer.2021.121717.

[9] B.V. Balakin, M. Stava, A. Kosinska, Photothermal convection of a magnetic nanofluid in a direct absorption solar collector, Sol. Energy 239 (2022) 33–39.

[10] S. Kumar, V. Sharma, M.R. Samantaray, N. Chander, Experimental investigation of a direct absorption solar collector using ultra stable gold plasmonic nanofluid under real outdoor conditions, Renew. Energy 162 (2020) 1958–1969.

[11] M. Karami, M. Akhavan-Bahabadi, S. Delfani, M. Raisee, Experimental investigation of cuo nanofluid-based direct absorption solar collector for residential applications, Renew. Sustain. Energy Rev. 52 (2015) 793–801.

[12] S. Delfani, M. Karami, M. Akhavan-Behabadi, Performance characteristics of a residential-type direct absorption solar collector using mwcnt nanofluid, Renew. Energy 87 (2016) 754–764.

[13] M. Alsaady, R. Fu, Y. Yan, Z. Liu, S. Wu, R. Boukhanouf, An experimental investigation on the effect of ferrofluids on the efficiency of novel parabolic trough solar collector under laminar flow conditions, Heat Transf. Eng. 40 (9–10) (2019) 753–761.

[14] P.G. Struchalin, D.M. Kuzmenkov, V.S. Yunin, X. Wang, Y. He, B.V. Balakin, Hybrid nanofluid in a direct absorption solar collector: Magnetite vs. carbon nanotubes compete for thermal performance, Energies 15 (5) (2022) 1604.

[15] K. Elsaid, A. Olabi, T. Wilberforce, M.A. Abdelkareem, E.T. Sayed, Environmental impacts of nanofluids: A review, Sci. Total Environ. 763 (2021) 144202, http://dx.doi.org/10.1016/j.scitotenv.2020.144202.

[16] A.B. Sengul, E. Asmatulu, Toxicity of metal and metal oxide nanoparticles: a review, Environ. Chem. Lett. 18 (2020) 1659–1683, http://dx.doi.org/10.1007/s10311-020-01033-6.

[17] X. Yuan, X. Zhang, L. Sun, W. Yuquan, X. Wei, Cellular toxicity and immunological effects of carbon-based nanomaterials, Part. Fibre Toxicol. 16 (2019) 18, http://dx.doi.org/10.1186/s12989-019-0299-z.

[18] G. Bystrzejewska-Piotrowska, J. Golimowski, P.L. Urban, Nanoparticles: Their potential toxicity, waste and environmental management, Waste Manage. 29 (2009) 2587–2595, http://dx.doi.org/10.1016/j.wasman.2009.04.001.

[19] R.E. Hewitt, H.F. Chappell, J.J. Powell, Small and dangerous? potential toxicity mechanisms of common exposure particles and nanoparticles, Curr. Opin. Toxicol. 19 (2020) 93–98, http://dx.doi.org/10.1016/j.cotox.2020.01.006.

[20] T. Ambreen, A. Saleem, C.W. Park, Thermal efficiency of eco-friendly mxene based nanofluid for performance enhancement of a pin-fin heat sink: Experimental and numerical analyses, Int. J. Heat Mass Transfer 186 (2022) 122451, http://dx.doi.org/10.1016/j.ijheatmasstransfer.2021.122451.

[21] S. Omiddezyani, V. Yousefi-Asli, E. Houshfar, S. Gharehkhani, M. Ashjaee, I. Khazaee, Investigation on the partial discharge characteristics of eco-friendly nanofluid insulation of corn oil nanofluid, Powder Technol. 378 (2021) 468–486, http://dx.doi.org/10.1016/j.powtec.2020.10.030.

[22] R. Sadri, M. Hosseini, S. Kazi, S. Bagheri, A.H. Abdelrazek, G. Ahmadi, N. Zubir, R. Ahmad, N. Abidin, A facile, bio-based, novel approach for synthesis of covalently functionalized graphene nanoplatelet nano-coolants toward improved thermo-physical and heat transfer properties, J. Colloid Interface Sci. 509 (2018) 140–152, http://dx.doi.org/10.1007/s42452-020-03259-z.

[23] M. Sarafraz, A. Arya, V. Nikkhah, F. Hormozi, Thermal performance and viscosity of biologically produced silver/coconut oil nanofluids, Chem. Biochem. Eng. Q. 30 (2016) 489–500, http://dx.doi.org/10.15255/CABEQ.2015.2203.

[24] S. Oparanti, A. Abdelmalik, A. Khaleed, J. Abifarin, M. Suleiman, O. VE, Synthesis and characterization of cooling biodegradable nanofluids from non-edible oil for high voltage application, Mater. Chem. Phys. 271 (2022) 125485, http://dx.doi.org/10.1016/j.matchemphys.2021.125485.

[25] S.M. Kumar, K.P. Viswanathan, S.H. Kumar, Investigation on the partial discharge characteristics of eco-friendly nanofluid insulation of corn oil nanofluid, IET Nanodielectrics 4 (2021) 130–142, http://dx.doi.org/10.1049/nde2.12020.

[26] N. Akram, R. Sadri, S.N. Kazi, S.M. Ahmed, M.N.M. Zubir, M. Ridha, M. Soudagar, W. Ahmed, M. Arzpeyma, G.B. Tong, An experimental investigation on the performance of a flat-plate solar collector using eco-friendly treated graphene nanoplatelets–water nanofluids, J. Therm. Anal. Calorim. 138 (2019) 609–621, http://dx.doi.org/10.1007/s10973-019-08153-4.

[27] L.H. Kumar, S. Kazi, H. Masjuki, M. Zubir, A. Jahan, C. Bhinitha, Energy, exergy and economic analysis of liquid flat-plate solar collector using green covalent functionalized graphene nanoplatelets, Appl. Therm. Eng. 192 (2021) 116916, http://dx.doi.org/10.1016/j.applthermaleng.2021.116916.

[28] M. Amar, N. Akram, G.Q. Chaudhary, S.N. Kazi, M.E.M. Soudagar, N.M. Mubarak, M.A. Kalam, Energy, exergy and economic (3e) analysis of flat-plate solar collector using novel environmental friendly nanofluid, Sci. Rep. 13 (2023) 411, http://dx.doi.org/10.1038/s41598-023-27491-w.

[29] E.C. Okonkwo, E.A. Essien, E. Akhayere, M. Abid, D. Kavaz, T.A. Ratlamwala, Thermal performance analysis of a parabolic trough collector using water-based green-synthesized nanofluids, Sol. Energy 170 (2018) 658–670, http://dx.doi.org/10.1016/j.solener.2018.06.012.

[30] V.K. Gupta, S. Kumar, R. Kukreja, N. Chander, Experimental thermal performance investigation of a direct absorption solar collector using hybrid nanofluid of gold nanoparticles with natural extract of azadirachta indica leaves, Renew. Energy 202 (2023) 1021–1031, http://dx.doi.org/10.1016/j.renene.2022.12.014.

[31] M. Alberghini, M. Morciano, L. Bergamasco, M. Fasano, L. Lavagna, G. Humbert, E. Sani, M. Pavese, E. Chiavazzo, P. Asinari, Coffee-based colloids for direct solar absorption, Sci. Rep. 9 (2019) 4701, http://dx.doi.org/10.1038/s41598-019-39032-5.

[32] F. Essa, A.H. Elsheikh, A.A. Algazzar, R. Sathyamurthy, M.K.A. Ali, M.A. Elaziz, K. Salman, Eco-friendly coffee-based colloid for performance augmentation of solar stills, Process Saf. Environ. Prot. 136 (2020) 259–267, http://dx.doi.org/10.1016/j.psep.2020.02.005.

[33] A. Kosinska, B.V. Balakin, P. Kosinski, Use of biodegradable colloids and carbon black nanofluids for solar energy applications, AIP Adv. 11 (2021) 055214, http://dx.doi.org/10.1063/5.0053258.

[34] A. Kosinska, B.V. Balakin, P. Kosinski, Photothermal conversion of biodegradable fluids and carbon black nanofluids, Sci. Rep. 12 (2022) 3398, http://dx.doi.org/10.1038/s41598-022-07469-w.

[35] B. Balakin, P. Struchalin, Eco-friendly and low-cost nanofluid for direct absorption solar collectors, Mater. Lett. 330 (2023) 133323, http://dx.doi.org/10.1016/j.matlet.2022.133323.

[36] V.K. Gupta, S. Kumar, R. Kukreja, Experimental investigation of a volumetric solar collector using natural extract of azadirachta indica based heat transfer fluids, Sustain. Energy Technol. Assess. 52 (2022) 102325, http://dx.doi.org/10.1016/j.seta.2022.102325.

[37] V. Popsueva, A. Lopez, A. Kosinska, O. Nikolaev, B. Balakin, Field study on the thermal performance of vacuum tube solar collectors in the climate conditions of western norway, Energies 14 (2021) 2745, http://dx.doi.org/10.3390/en14102745.

[38] Regulus, Solar system with kpg1-alc collectors, 2023, installation and operation manual (last visit date 22.03.2023), https://www.regulus.eu/download/navody/nn_en_navod_navod-slunecni-kolektor-kpg1-alc.pdf.

[39] A.S. for Testing, Materials, Astm g-173-03, 2023, standard terrestrial solar spectral irradiance distributions (last visit date 22.03.2023), https://www.nrel.gov/grid/solar-resource/assets/data/astmg173.xls.

[40] J.A. Duffie, W.A. Beckman, Solar Engineering of Thermal Processes, John Wiley & Sons, 2013.

[41] C. Scientific, SP Lite 2 pyranometer. instruction manual, https://s.campbellsci.com/documents/ca/manuals/splite2_man.pdf.

[42] E.A.C. Panduro, F. Finotti, G. Largiller, K.Y. Lervåg, A review of the use of nanofluids as heat-transfer fluids in parabolic-trough collectors, Appl. Therm. Eng. 211 (2022) 118346.

[43] R. Brechner, G. Bergeman, Contemporary Mathematics for Business & Consumers, Cengage Learning, 2016.